ROLE OF ENERGY DISSIPATION AND SURFACE MOBILITY IN HETEROGENEOUS CATALYSIS BY METALS

Zlatko KNOR[1] and Jan PLSEK[2]

J. Heyrovsky Institute of Physical Chemistry, Academy of Sciences of the Czech Republic, 182 23 Prague 8, Czech Republic; e-mail: [1] knor@jh-inst.cas.cz, [2] surfaces@jh-inst.cas.cz

Received May 15, 1998
Accepted July 20, 1998

The fundamental role of excess energy dissipation and of surface species mobility, both in the preparation of model metallic catalysts (bimetallic catalysts, bimetallic oxide-supported catalysts), and in the activation of reactant molecules on the catalyst surfaces (single crystals, bimetallic and bimetallic oxide-supported catalysts) are discussed. A generalized model of surface interactions is proposed which satisfactorily explains the trapping of particles from the gas phase at the atomic steps and recovery of the trapping sites due to migration of the trapped species towards flat terraces. Higher probability of encounter of these species with other reactants on flat terraces and easier desorption of the reaction products from there in comparison with the bound state at the edges of atomic steps can be expected. Results of FIM and FEM studies of Pt, Dy–W, Pd–W and Pd–Mo systems are used to illustrate selected features of the proposed general model.

Key words: Surface mobility; Energy dissipation; Trapping sites; Catalysis by metals; Reaction zone; Field emission microscopies; Heterogeneous catalysis.

Interaction of one particle (atom of a growing lattice or a reactant molecule) with a metallic surface can be generally described by a potential energy hypersurface. Construction of such a multidimensional dependence of the interaction energy on the coordinates of all the species involved in this interaction represents an immense task. Therefore, many authors limit themselves to one-dimensional (1D) approximation, *i.e.*, a single particle approaching perpendicularly the solid surface. For molecules, an additional restriction is usually adopted, *viz*. a fixed orientation of the molecule with respect to the surface plane[1]. This 1D approach can be represented by a potential energy (*PE*) curve (the energy of interaction between the particle and the surface (*E*) as a function of the particle–surface distance, *z*). For diatomic molecules, a more exact representation can be used, namely, the *PE* surface $E(d,z)$, where d is the intramolecular bond length and z again the perpendicular molecule–surface distance. However, both $E(z)$ and $E(d,z)$ are valid only for one particular point on the solid surface (the target site, the particle is aiming at). Understandably, different target sites are characterized by different *PE* curves (*PE* surfaces). The same conclusion also holds for the sites

occupied and unoccupied by the previously trapped particles. All the preceding statements are valid for the general *PE* hypersurfaces, too.

Figure 1 depicts particles M_i approaching different sites S_i along the line x on a surface (a) and a set of the corresponding *PE* curves (b). For example, *PE* curve in the plane σ_1 represents the head-on-head collision of the particle M_1 with a surface atom S_i and *PE* curve in the plane σ_2 corresponds to the case when the particle M_2 is aiming at the middle point within the gap between the two surface atoms S_i and S_{i+1} (Fig. 1). Figure 1b also shows the section through the minima of this "*PE* surface". The deepest minima (adsorption sites) are separated by *PE* barriers V_{0w} (activation energies for surface migration). The curve $E(Z_0,x)$ connecting the minima of individual *PE* curves (Fig. 1), corresponds to an ideal (homogeneous) surface, where the adsorption sites and activation barriers between them are identical over the whole surface. However, even a densely populated (atomically flat) plane of a single crystal is far from being ideal. Many defects occur on it: atomic steps with kink sites and corners, vacancies, *etc*. (Fig. 2). The "chemical unsaturation" of surface atoms at such defects results in a stronger interaction with gas molecules. In analogy with the crystal growth, one can expect that these sites act as trapping sites for gas molecules, too. The number of particles striking a unit surface area per unit time is of course constant all over the surface at the given conditions. However, the trapping (chemisorption) of a particle can be expected as more probable at the "unsaturated" atoms (at the edges of atomic steps), than at sites on flat terraces. This is understandable because the dissipation of energy (excess kinetic energy, adsorption heat) by phonons, surface reconstruction or by local excitation of metal electrons is probably easier at atomic steps compared with atomically flat terraces (Fig. 3). Moreover, the sites at the edges of atomic steps are charac-

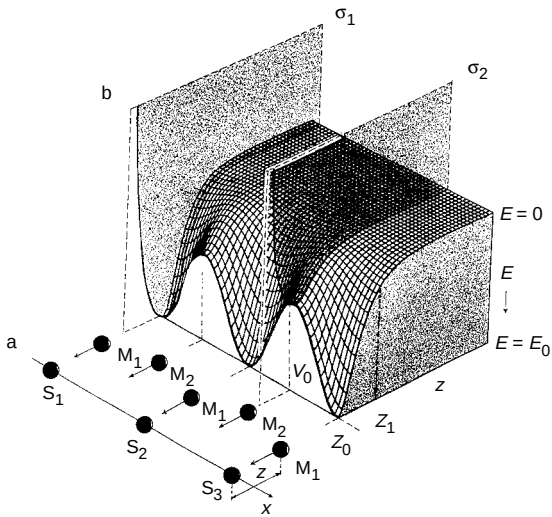

FIG. 1
A set of one-dimensional *PE* curves $E(z)$ (b), which represent the interaction of individual molecules M_i, approaching perpendicularly the solid surface, in the form of a linear chain of surface atoms Si_i (a). E is the potential energy of interaction between a single molecule and the surface (for a particular target site); far from the surface $E \rightarrow 0$ and for the molecule trapped in the equilibrium distance above the surface (at the point Z_0), $E = E_0$. $E(z)$ might result from a quantum mechanical calculation or a semiempirical potential can be used (*e.g.*, the Morse potential). Further details of this figure are explained in the text

terized (due to their "chemical unsaturation") by deeper *PE* wells. According to the Frenkel equation[2] for the mean sojourn time of a particle at the surface, this means that the particle resides on these sites for a long time period. Thus the probability of the excess energy loss is further increased (Fig. 4).

Molecules trapped at the edges of atomic steps will be probably strongly perturbed both due to the localized interaction with surface atoms and due to screening (Fig. 3). The effective screening close to the atomic steps can be understood in terms of the Smoluchowski smoothing effect of electrons at the edges of atomic layers (see, *e.g.*, ref.[3]). Such a perturbation might result even in a complete dissociation of, *e.g.*, diatomic molecules.

Any chemical interaction is governed by the outermost electrons of chemically interacting species, in our case of the reactant molecules and of the metal surface. The binding energy of outermost electrons corresponds for molecules to their ionization energy (I) and for the metal surfaces to their work function (φ). I = 13–15 eV for simple diatomic molecules and φ = 4–6 eV for transition metal surfaces. Consequently, when a molecule approaching a metal surface (Figs 3a–3c) is close to its "bonding" distance $\approx$ 0.1 nm (minimum of the *PE* curve), then, due to the exchange and correlation repulsive forces, a hole is created in the electron charge density (Figs 3b and 3c). This process might be considered as one of the channels for dissipation of the excess kinetic energy of the impinging molecule. At this moment, the molecule starts to interact with the localized "atomic-like" states of the surface atoms[4–6] (Figs 3d and 3e). This type of states at the surface atoms of the transition metals has been evidenced by the field ion microscopy[4–6] (FIM) (similar conclusions resulted from the theory of the scanning tunneling microscope[7], STM). These "atomic-like" states need not exist at the surface atoms permanently. The "outermost" states of surface atoms are probably hybridized

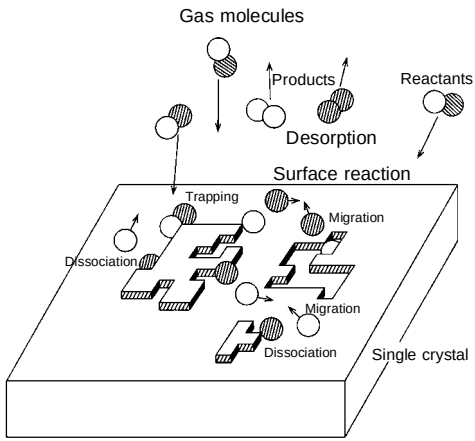

FIG. 2
Schematic view of elementary steps of a catalytic reaction, taking place on a single crystallographic plane of a metal, where two types of defect sites (atomic steps, vacancies) are shown

along the surface plane (in analogy with π-type bonds in ordinary chemical compounds). A particle approaching the surface from the gas phase perturbs this hybridization and "atomic-like" states are created as precursors to a "chemical" bond. This model can be successfully applied to the metal-crystal growth from the gas phase as well as to chemisorption of molecules[5] or field ionization of inert gas atoms in FIM (ref.[6]).

During the time spent by the molecule (selectively perturbed by the formation of localized bonds with the surface atoms) in the trapped state its outermost electrons become a part of the electron system of the crystal and the charge density of metal electrons relaxes to a new spatial distribution. The molecule becomes partially or completely immersed into the Fermi sea of metal electrons (Figs 3d and 3e). The mean sojourn time of a molecule in a weakly chemisorbed state is between 10^{-3} and 10^{-1} s,

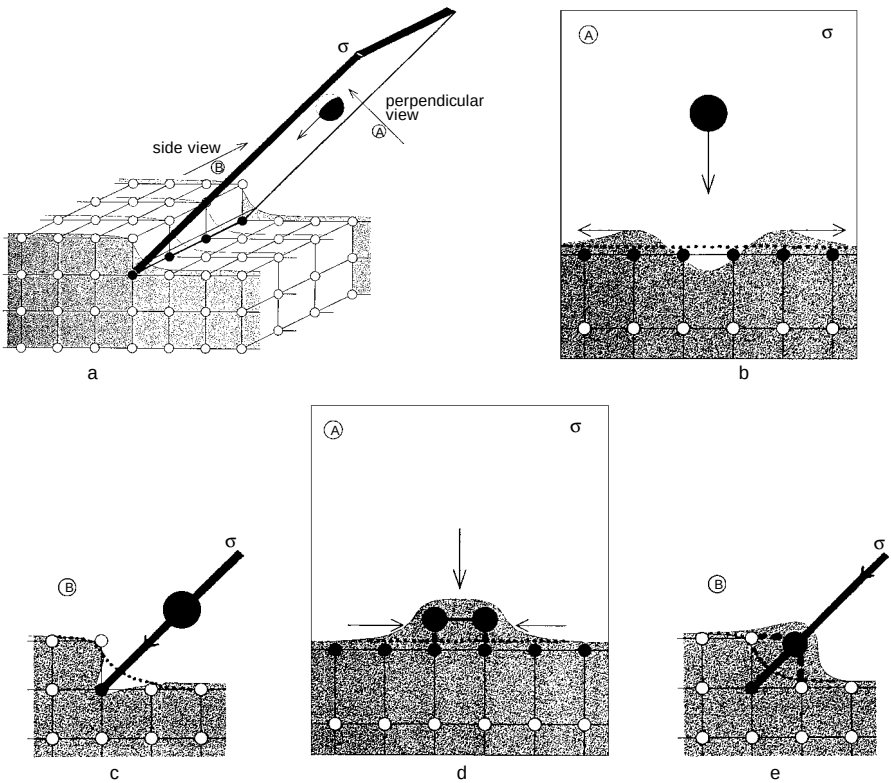

FIG. 3

Model of the interaction of a diatomic molecule with an atomic step on a transition-metal surface[5]. Molecule (black sphere) approaches perpendicularly the step along the plane σ (a). The contours of the electron charge density are schematically shown (grey region). Small circles represent ion cores, forming the crystal lattice. The front views A (projection into the σ plane) and side views B, illustrating different stages of the interaction, are shown in (b, d) and (c, e) parts, respectively (for details see the text)

and the life-time of the electron-hole excitation is $\approx 10^{-11}$ s. Due to the screening effects, this "embedding" of a molecule into the charge density at the metal surface results in weakening of both the intramolecular bonds (leading eventually to a total dissociation) and of the localized bonds of the molecule (or of its fragments) with the surface atoms[5] (Figs 3d and 3e). Relaxation of the electron charge density is thus responsible for: (i) dissociation of the reactant molecules trapped at atomic steps or other surface defects; (ii) weakening of bonds between the fragments (atoms) and metal atoms, enabling them to migrate away from edges of the atomic steps*. Due to this effect, the original trapping sites are again ready for trapping further reactant molecules.

Up to this point we have discussed the elementary steps of a catalytic process on a single-component surface. In the case of a multicomponent, *e.g.*, bimetallic, surface, an additional condition for its successful operation has to be fulfilled, *viz.* that the individual components have to "cooperate" in some way. If the individual elementary steps proceed separately on individual components of the surface, the simplest kind of "cooperation" between them would be migration of perturbed reactant molecules (or their fragments) from one component to the other, where further reaction could take place (Fig. 5).

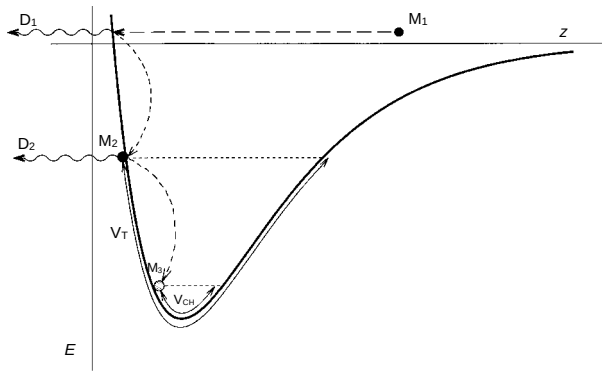

FIG. 4

PE curve $E(z)$ for a molecule M_1 approaching a trapping site at an atomic step. The loss of its excess kinetic energy *via* dissipation channel D_1 (which might correspond to Figs 3b and 3c) causes its trapping in the M_2 state. There it vibrates (V_T) for a certain time period, without chance to leave this potential well. Its life time in this state can be long enough so that further excess energy could be dissipated and the molecule would end up in the chemisorbed state M_3

* Theoretical arguments in favour of the above formulated elementary stages of a catalytic process, occurring on transition metal surfaces, particularly the effect of immersing the diatomic molecule into a non-zero charge density, can be found in Berlin's formulation of the Hellmann–Feynman theorem[5,8].

In the preceding paragraphs, the fundamental role of excess energy dissipation and of surface species mobility (trapped and perturbed reactant molecules or their fragments) in catalysis by transition metals has been demonstrated. In what follows, an experimental evidence is presented for various types of mobility and their manifestation in the phenomena observed on transition metal surfaces. The following topics will be discussed: (i) mobility of metal atoms along the surface plane and perpendicularly to it (possible formation of a surface alloy) which are important for preparation of well defined model catalysts; (ii) mobility of reactant molecules and/or of their fragments (atoms) on single crystals and on the oxide-supported bimetallic model catalysts.

EXPERIMENTAL

Experiments have been performed sequentially in two equipment: (i) in a home-made ultra-high vacuum (UHV) all-glass apparatus with glass cells for a field emission microscope (FEM) and a field ion microscope[10] (FIM), (ii) in FEM and FIM built into a commercial stainless-steel apparatus USU 4 (U.S.S.R. provenance) (ref.[11]). The latter apparatus was further equipped with a turbomolecular pump and a quadrupole mass spectrometer (Balzers, Liechtenstein). The vacuum chamber was connected *via* a sapphire leak-valve (Varian, U.S.A.) to a home-made all-glass gas-handling system[10,11]. Other details of the above-mentioned equipments, as well as the used experimental procedures were described earlier[10,11].

RESULTS AND DISCUSSION

Role of Surface Mobility of the Metal Atoms in Preparation of Bimetallic Model Catalysts

The first bimetallic systems investigated in our FEM were prepared by evaporation of palladium in UHV onto a clean tungsten tip. Figure 6 shows the results of such an experiment. Palladium layer was deposited at $T \approx 78$ K from the left-hand side perpen-

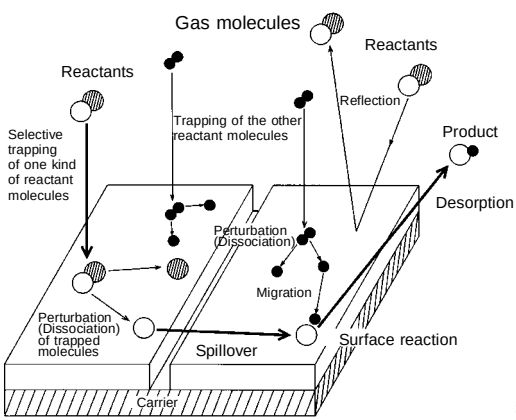

FIG. 5
Scheme of a surface reaction occurring on a supported bimetallic catalyst

dicularly to the tip axis. Since the average work-function values are[12]: $\overline{\varphi_{Pd}}$ = 5.6 eV for a polycrystalline palladium film and $\overline{\varphi_W}$ = 4.5 eV for a tungsten tip, respectively, the Pd layer slightly darkens the FEM image. Under such conditions, one would expect that the image of clean tungsten (Fig. 6c) would change so that a sharp boundary would

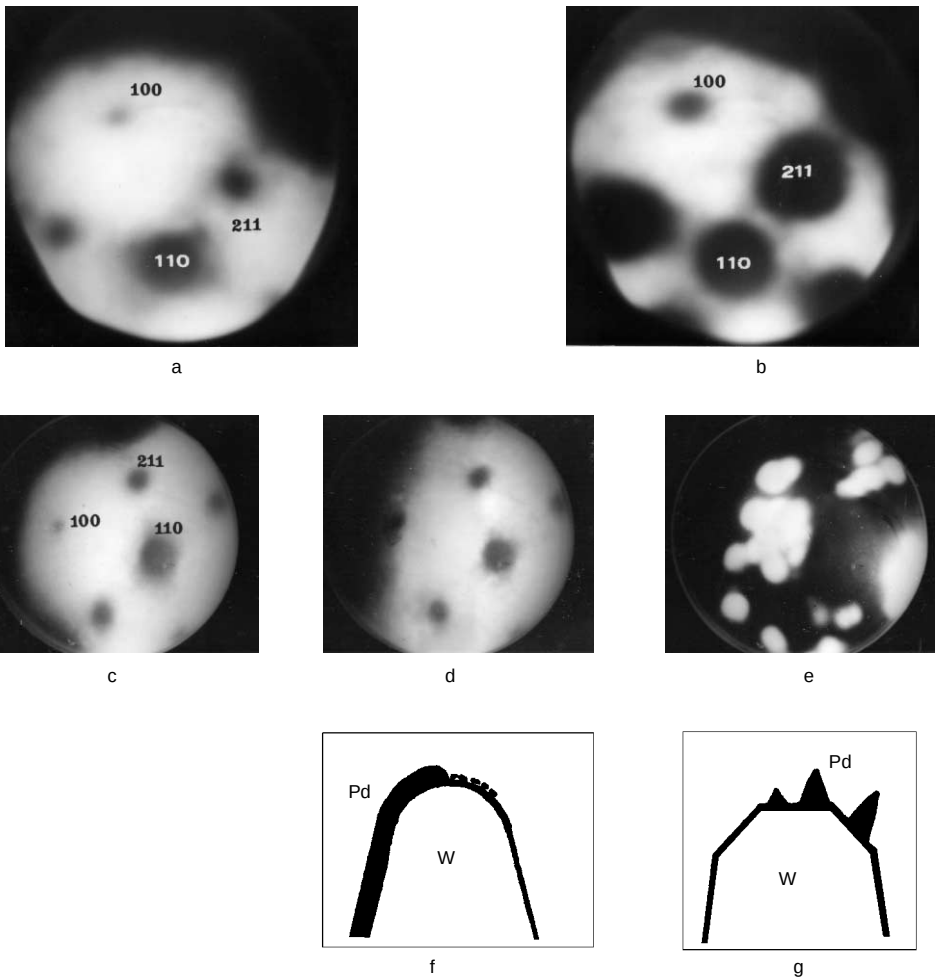

FIG. 6

FEM images of a bare and Pd-covered tungsten tip. Comparison of the results of the high-temperature, high-field treatment of: (i) a clean tungsten tip and (ii) a tungsten tip covered by a Pd layer: a thermally cleaned tungsten surface (repeated flashes up to $T \approx 2\ 600$ K), imaging voltage 4.7 kV; b after 2 min at $T \approx 1\ 800$ K in the presence of the field of the order of 10^9 V/m; c thermally cleaned tungsten surface (imaging voltage 11 kV); d Pd layer deposited at 78 K onto the tip from the left-hand side (imaging voltage 11 kV, ref.[20]); e after 1 min at $T \approx 1\ 400$ K in the presence of the field of the order of 10^9 V/m; f and g are schematic side views of the tip relevant to d and e

divide the image into two parts, the left-hand part (corresponding to the deposited Pd layer) becoming dark and the right-hand part (corresponding to the free tungsten surface) remaining bright. In reality, however, the whole surface becomes dark, *i.e.*, it is covered by palladium, though on the right-hand side obviously by a monolayer only (the original pattern of tungsten is still visible there) (Fig. 6d). Going to the left the brightness is continuously decreasing, probably because of the increasing thickness of the palladium layer (*cf.* Figs 6c and 6d with the scheme 6f). This change of the FEM image was definitely not caused by adsorption of residual gases (which might evolve from the palladium source), as proved by the negative result of a blank experiment (the glass shutter of the evaporator was closed, while the Pd source was running). Obviously, the high kinetic energy of some Pd atoms (the temperature of the Pd source was $T \approx 1\ 500$ K) was not efficiently dissipated into the cooled tip and individual Pd atoms could thus reach the "shadow" side of the tip apex. This can be understood if one assumes that the Pd atoms are trapped at a larger distance Z_1 from the surface (Fig. 1b) (because of their high kinetic energy). At this distance the *PE* minima are less deep and the activation barriers are lower than at the equilibrium distance Z_0 (Fig. 1b). Palladium atoms can thus move more or less freely along the surface.

Figure 6d shows the early stage of the Pd deposition. If the deposition continues (Fig. 7a), a thick layer of palladium finally results which exhibits a stepped boundary, with radii of curvature smaller than that of the apex itself. Then, due to high intensity of the electric field at this region (see the following Note), it is imaged in the form of

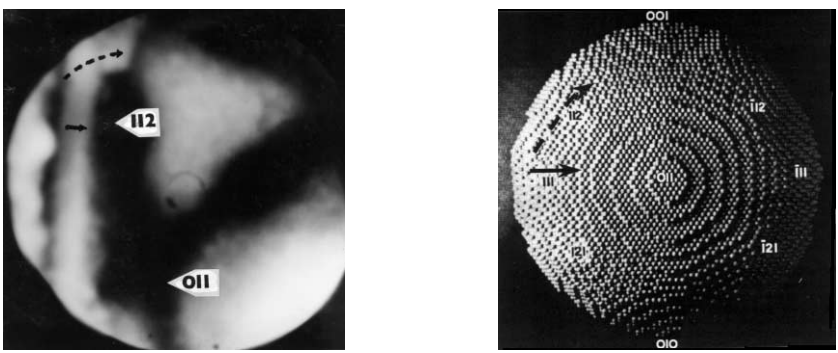

a b

FIG. 7

FEM image of a thick layer of palladium deposited at 78 K onto the tungsten tip from the left-hand side (imaging voltage 6.5 kV, ref.[25]) and heated for several seconds to $T \approx 300$ K (a), and a ball model of the tungsten-tip apex[15] (b). The full arrow shows the route, characterized by high activation barriers (across the ridges and troughs), whereas the dashed line arrow shows the route with low activation barriers (along the flat terraces)

bright strips at the left-hand side of the FEM image (Fig. 7a) though $\overline{\varphi_{Pd}} > \overline{\varphi_W}$. In contrast to the preceding case, surface migration of a thick layer at a higher temperature proceeds from the equilibrium states, *i.e.*, the Pd atoms follow the route starting from the deepest minima (see Fig. 1b). Consequently, the edge of the thick Pd layer starts to move along the way which exhibits smallest activation barriers, *i.e.*, along the terraces (see the dashed arrow in Figs 7a and 7b, the latter showing the ball model of the apex of the W tip). The route (indicated by a full arrow) which would cross perpendicularly the ridges and troughs of the (112) plane of tungsten covered by a Pd monolayer is avoided because it would require to overcome the high potential barriers.

Migration of surface species is strongly influenced not only by the topographical features of the solid surface, but also by its chemical nature. If, for example, the energy of the mutual interaction (E_{AA}) of the deposited metal atoms is smaller than their interaction energy with atoms of the supporting substrate (E_{AS}), the low-temperature deposition of such a metal results in an amorphous layer which does not recrystallize even after heating to a higher temperature. As an example can serve FIM image showing the random structure of a dysprosium layer deposited onto the tungsten tip[13] (in the "head-on-head" direction) (Fig. 8b). By contrast, if $E_{AA} > E_{AS}$ (Pd layer deposited onto the tungsten tip) and the deposited layer is thermally aged, formation of a polycrystalline layer can be observed in FIM (ref.[13]) (Fig. 8c). This interpretation is supported by the values of the vaporization enthalpies[14], $\Delta H_{Dy} = 2.9$ eV and $\Delta H_{Pd} = 3.88$ eV and by the

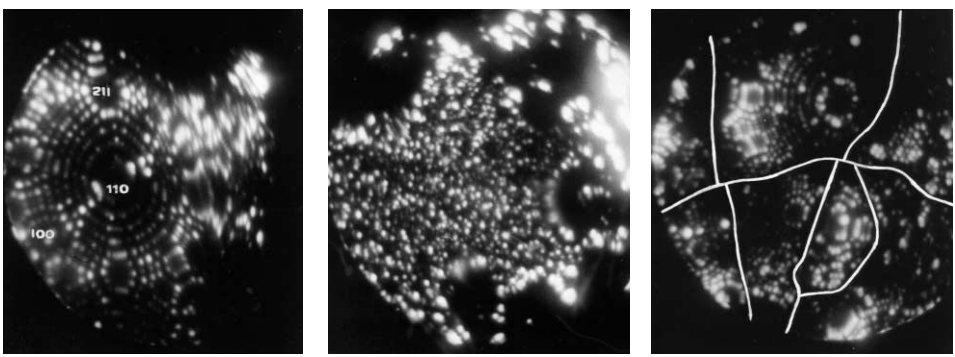

FIG. 8

FIM images of: a tungsten tip (imaging gas was He, $T \approx 78$ K, imaging voltage was 10.6 kV); b dysprosium layer deposited "head-on-head" onto the apex of the W tip (imaging gas was Ar, $T \approx 78$ K, imaging voltage was 7.7 kV); c polycrystalline palladium layer deposited "head-on-head" onto the apex of the W tip (the grain boundaries were visualised by white lines) (imaging gas was Ne, $T \approx 78$ K, imaging voltage was 9.7 kV, ref.[13])

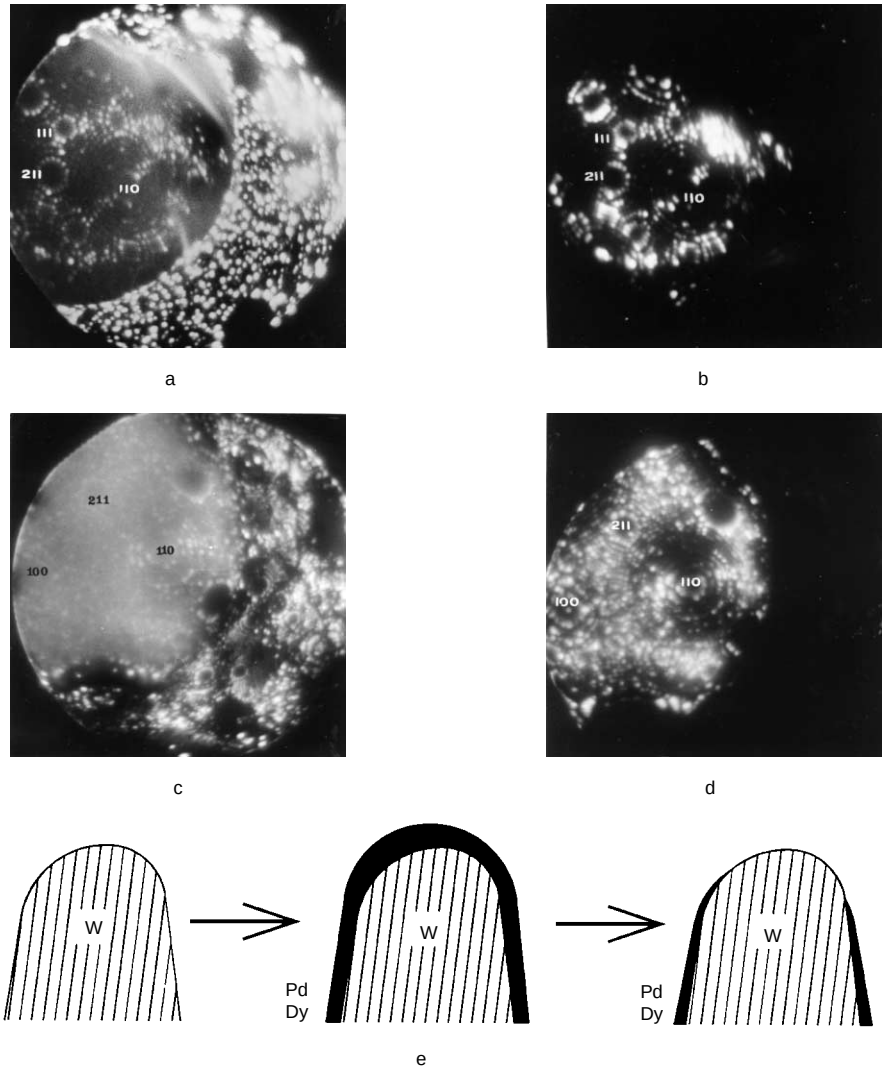

FIG. 9

FIM images of: a dysprosium layer, partially field-evaporated from the tip apex (see the schematic side view of the tip e, during this process) so that the structure of the underlying tungsten is visible (imaging gas was Ar with admixture of He, $T \approx 78$ K, field-evaporation voltage was 13.8 kV, imaging voltage was 11.8 kV); b the same surface as in a, imaging voltage being 5.3 kV (Ar image of the bare part of tungsten); c a palladium layer, partially field-evaporated from the tip apex so that the structure of the underlying tungsten is again visible (imaging gas was Ne, field-evaporation voltage was 12.7 kV, imaging voltage was 12.4 kV); d the same surface as in c, imaging voltage being 9.3 kV (for obtaining a sharp image of the "bare" surface which was dim in c, ref.[13])

voltages, needed for the field-evaporation of dysprosium and palladium layers from the tungsten tip (Fig. 9)*.

Information on the vertical diffusion (incorporation) of deposited atoms into the substrate lattice is presented for the investigated systems (Dy/W and Pd/W) in Fig. 9. In the case of a partially field-evaporated Dy layer (as shown schematically in Fig. 9e) a well developed structure of the free tungsten surface with a sharp boundary can be seen in the left-hand part of the FIM image[13] (Figs 9a and 9b). On the other hand, when the Pd layer is partially field-evaporated, the structure of the "free" tungsten surface (Figs 9c and 9d) exhibits some irregularities together with a "diffuse" boundary[13]. During the thermal aging of the Pd/W system which is needed for obtaining well developed structure of the Pd crystallites, a part of Pd atoms has been obviously incorporated into the surface layer of tungsten (surface alloy formation) and thus the obtained image does not correspond to the structure of a clean tungsten surface[13]. Formation of Pd–W surface alloy and exclusion of such phenomenon in the Dy/W system correlates well with sizes (covalent radii R) of these atoms: R_{Dy} = 0.16 nm (ref.[16]), R_{Pd} = 0.13 nm (ref.[17]) and R_W = 0.14 nm (ref.[18]).

The mentioned effect of the chemical nature of the interface between two metals is even more pronounced in the case of metal–oxide–metal (MOM) systems. These systems were introduced for FEM and FIM studies in this laboratory** as models of commercial oxide-supported single-metallic and bimetallic catalysts[19,20].

The first MOM systems were obtained by a heavy oxidation of tungsten tips which were subsequently partially covered by a Pd layer[19], deposited from the right-hand side (in the same FEM as in Fig. 6d, where, however, Pd was deposited onto the clean tungsten tip from the left-hand side). In contrast to Fig. 6d, a sharp boundary of the Pd layer was obtained in this case (Fig. 10c), obviously because of the increased sticking

* From the general point of view, the quantity that should be in this case compared is intensity of the field at the apex. This intensity is proportional to the ratio U/R (U being the applied evaporation voltage and R being the apex radius)[15]. From simple geometric considerations, one can conclude that the apex radius for a BCC metal is equal to 2 d (d being the distance between the centers of the (211) and (110) planes). As can be seen from Figs 9b and 9d, the radius of the Dy-covered apex is smaller than the radius of the Pd-covered apex. Consequently, the intensity of the field which is needed for evaporation of Dy is higher than the intensity for evaporation of Pd indeed.

**During the experiments with such MOM systems, an unusually high electron emission has been observed which was comparable or even higher than that of the original clean tungsten tip. This effect has been attributed to the resonance-enhanced tunneling[22–24]. If the external metallic layer is prepared by the vapour deposition of a chemically inert metal (*e.g.*, gold), a high stability of the electron emission can be achieved[22]. Such a MOM system appears thus to be a promising candidate for construction of a stable point source of electrons (exhibiting additionally an extremely narrow energy distribution) suitable for high-resolution transmission electron microscopes and spectrometers for electron energy-loss measurements.

probability of Pd atoms on the WO_x surface. Another factor which might play some role in the formation of the metal-oxide boundary is the mutual wettability: a good wettability in the metal-on-metal systems and poor in the metal-on-oxide systems can be expected[21].

The observation of a sharp boundary after low-temperature deposition of a late transition metal (Pd) onto the WO_x surface does not seem to be chemically specific: the same sharp boundary was observed with the low-temperature deposition of an early transition metal Mo (Fig. 10d). The two groups of metals, however, differed considerably when the deposited layers were heated to higher temperatures[20]. In the case of Mo, chemical reaction with a surface oxide layer took place, succeeded by MoO_3 dissolution in the WO_x layer or its sublimation in vacuum (see identical FEM images, Figs 11b and 11d). On the other hand, Pd exhibited an ordinary sintering effect (Figs 11f and 11g), typical of dispersed metals.

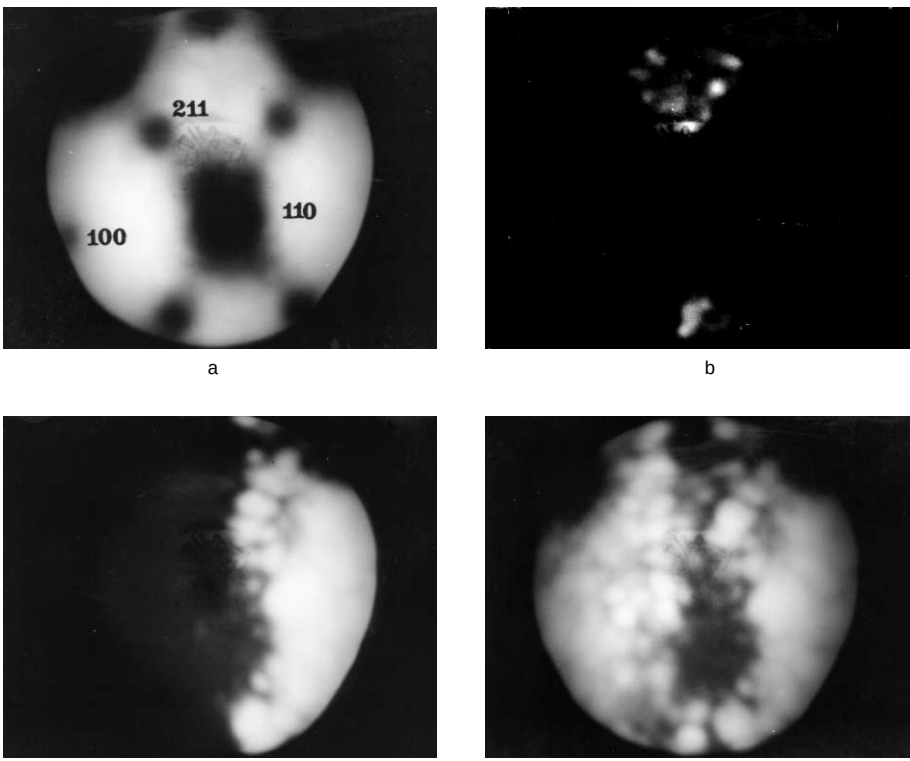

FIG. 10

FEM images of: a clean tungsten (imaging voltage was 3 kV, $T \approx 78$ K); b heavily oxidized surface[6] (imaging voltage was 4.1 kV, $T \approx 78$ K); c palladium deposited from the right-hand side at $T \approx 78$ K (imaging voltage was 4.1 kV, $T \approx 78$ K); d molybdenum deposited at $T \approx 78$ K onto the surface under c from the left-hand side (imaging voltage was 4.1 kV, $T \approx 78$ K, ref.[6])

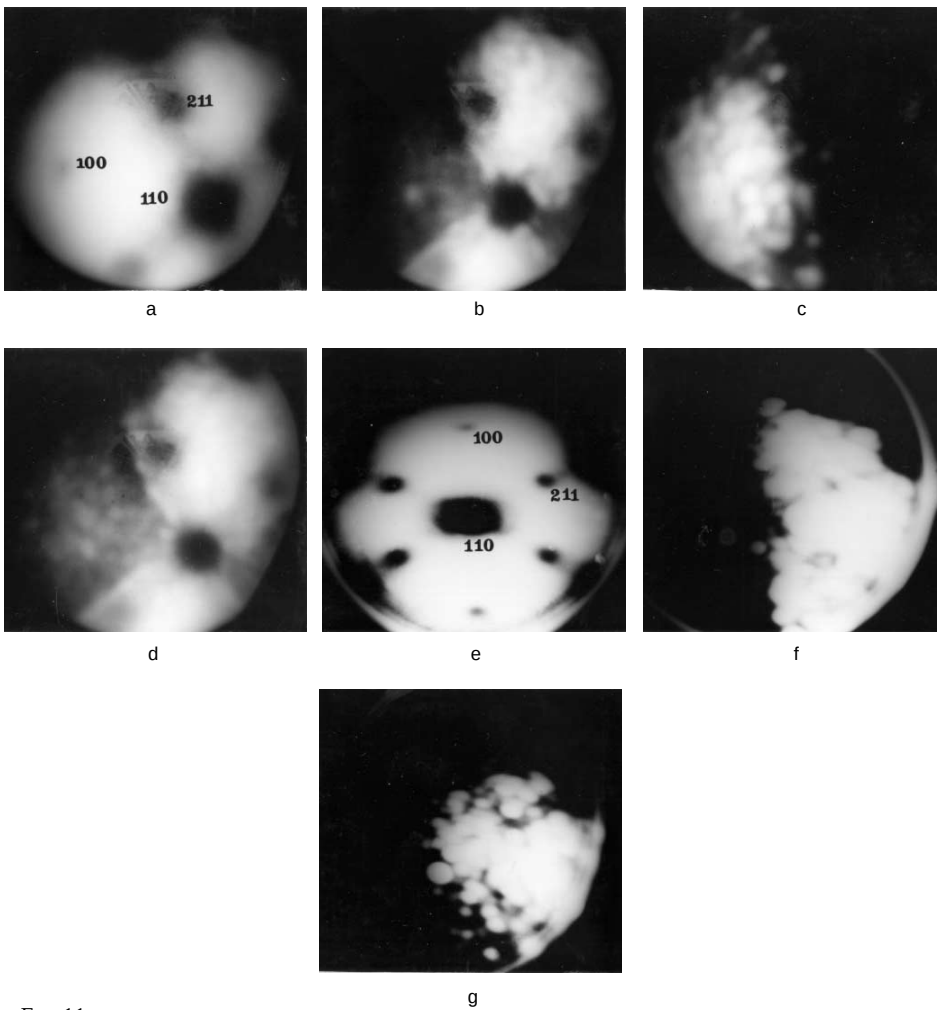

FIG. 11

FEM images of: a clean tungsten surface (imaging voltage was 3.4 kV, $T \approx 78$ K); b oxidized tungsten surface[20] (imaging voltage was 5.4 kV, $T \approx 78$ K); c molybdenum deposited at $T \approx 78$ K onto the tip apex from the left-hand side (imaging voltage was 3.6 kV, $T \approx 78$ K); d the tip heated for about 3 s to $T \approx 1\ 200$ K, ref.[20]); e clean tungsten surface (imaging voltage was 6 kV, $T \approx 78$ K); f palladium layer deposited from the right-hand side onto an oxidized tungsten surface (imaging voltage was 7.5 kV); g the tip heated for about 1 s to $T \approx 1\ 200$ K (imaging voltage was 7.5 kV, $T \approx 78$ K, ref.[19])

The MOM systems still exhibited an interesting feature, namely that the WO_x layer was able to prevent the Pd atoms from vertical diffusion into the underlying tungsten lattice, in contrast to the case, when the Pd layer was in direct contact with the bare tungsten surface[19].

The non-stoichiometric tungsten oxide in the above described experiments was probably a semiconductor. It was therefore interesting to investigate also a typical insulator as an oxide interlayer in the MOM system. With Al_2O_3 (which is also a typical carrier in the catalysis by supported metals) similar results to those of the WO_x interlayer were obtained[11].

Surface Mobility of Perturbed Reactant Molecules and/or of Their Fragments

Single component surfaces. The extraordinary shape of the sample in FEMs and FIMs, *viz*. a single crystal etched into an extremely sharp tip (with the end curvature radius of 10^2 to 10^3 nm) makes it possible to investigate the ability of perturbed reactant molecules or of their fragments to migrate from the trapping sites at the edges of atomic steps towards the "reaction region" on terraces where they can more or less freely move around. The probability of their collision with other reactants is thus increased in comparison with the state bound at the step (see Fig. 2)*. Moreover, attractive interaction might become operative on flat terraces and also desorption of product molecules from there might be easier than their desorption from edges of the atomic steps. The above mentioned mechanism of a surface reaction can be successfully studied in FEM, provided the trapping sites exist only in a specific region of the sample surface. The location of such a region can be then identified from the initial shape of the reaction zone, if two conditions are fulfilled: (i) the rate of the reaction should be low to make the initial shape of the reaction zone observable, (ii) the surface mobility of the reactants should be limited, in order not to smear out the original anisotropy of the trapping sites distribution. These two conditions can be fulfilled if the investigated reaction is performed at an appropriately low temperature. The region around the Pt (111) plane is an example of such a surface with well defined trapping regions[5,6,26,27] which form three sectors around the (111) plane, separated from each other by another three "inert" sectors.

Figure 12 demonstrates that, in this favourable case, the distribution of the trapping sites on the above specified Pt surface can be judged from the anisotropy of the reaction zone indeed.

Multicomponent surfaces. Migration of trapped reactant species in multicomponent systems is called a spillover effect. The first experimental evidence of this effect was

* The latter statement is correct for surface reactions of the Langmuir–Hinshelwood type only. Since the Rideal–Eley type of reactions is very rare, it is, however, almost generally applicable.

presented at the 3rd International Congress on Catalysis in Amsterdam 1964 for hydrogen and platinum[28] and for hydrogen and nickel[29] (the latter evidence was not perceived by most of the later authors[30,31], though it has been performed under better defined conditions).

If mobility of reactants or of their fragments on Pd–W surfaces in FEM should be investigated, a visible sharp boundary between the palladium and tungsten regions would be required. This goal can be achieved by high-temperature treatment in a high electric field[25], chosen so that the shape of the tungsten tip only slightly changes from a hemispherical (high-temperature equilibrium) shape into a polyhedral[32], with increased size of low index planes (100), (211) and (110) (Figs 6a and 6b). On the other hand, in the bimetallic system Pd–W, even under milder conditions, small Pd microcrystals grow (due to the higher polarizability of Pd atoms and lower cohesion of Pd metal compared to W) (Fig. 6e). Details of the preparation of such a sharp Pd–W boundary are described in ref.[25]. Because of small end curvature radius of these Pd microcrystals (and, consequently, a higher electric field in their apex vicinity) they appear as bright spots on the FEM image (Figs 6e and 6g) (a similar effect as in the case of stepped boundary of thick Pd layers, Fig. 7a).

The Pd–W system described in the preceding paragraph (Figs 6e and 6g) when contacted with nitrogen gas is suitable for direct investigation of the spillover of reactant fragments on bimetallic surfaces (because Pd is not able to trap and dissociate the nitrogen molecules at room temperature in contrast to tungsten)[25]. Figure 13 presents results of this study. Under the above described experimental conditions the tungsten surface is fully covered by chemisorbed layer of nitrogen atoms and the palladium surface is completely free. Since the binding energy of nitrogen atoms to the W surface, (calculated from the initial heat of nitrogen adsorption on W, Fig. 14) is about 7 eV while on Pd it is 4 eV only, one can ask what the driving force for the migration of nitrogen atoms from the tungsten to the palladium surface is. Figure 14 demonstrates that the adsorption heat of nitrogen on tungsten falls down with increasing coverage, so

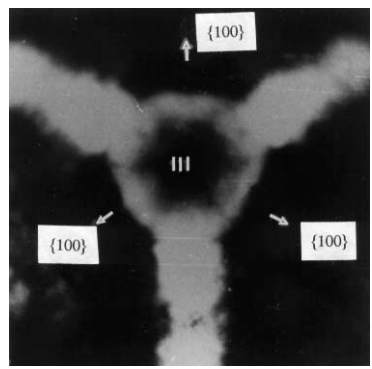

FIG. 12
FEM image of the initial shape of the reaction zone (bright region) around the (111) plane of platinum for the reaction of H_2 with preadsorbed oxygen at $T \approx 115$ K (ref.[27])

that at full coverage it corresponds to the binding energy of nitrogen atoms lower than 4 eV. We can thus conclude that the driving force for nitrogen migration from W towards Pd at room temperature is the concentration gradient only.

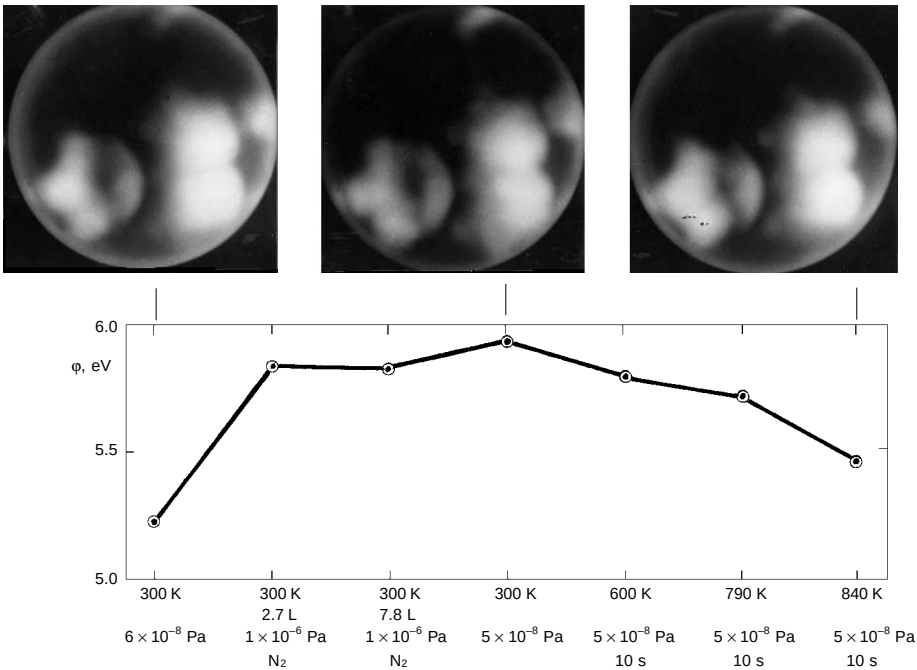

FIG. 13

The average work function values (φ) for Pd microtips exposed to nitrogen gas (pressure 1×10^{-6} Pa), after pumping nitrogen away and after thermal desorption. The inserted FEM images of Pd microtips correspond to the initial, intermediate and final states of the Pd surface, respectively (L = langmuir, ref.[25])

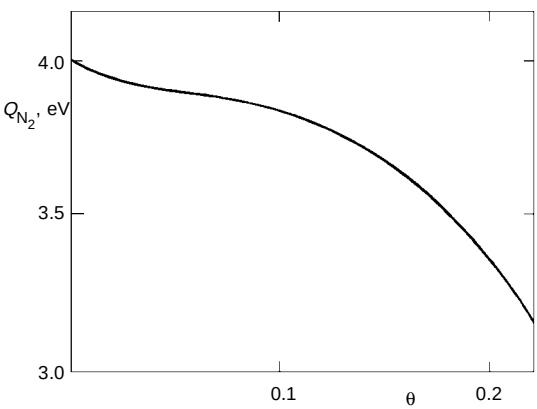

FIG. 14

Heat of nitrogen chemisorption Q_{N_2} as a function of coverage Θ (ref.[33]). Binding energy of nitrogen atoms with the surface $E_{N–Me}$ has been calculated according to the approximate equation[9]: $E_{N–Me} = (Q_{N_2} + D_{N–N})/2$ ($D_{N–N}$ = 9 eV is the dissociation energy of a nitrogen molecule)

Similarly, the spillover of nitrogen atoms on the analogous oxide-supported Pd–Mo/WO_x system (described above, see Fig. 10d) was well documented[10]. An additional factor could be investigated in this MOM system, namely the size of the gap (the distance) between the Pd and Mo islands (clusters). Understandably, nitrogen atoms prefer to migrate along the shortest way across the oxide surface between metallic islands (approximately 1 nm). Migration across the gaps broader than about 2 nm was not observed[10]. This study of oxide supported Pd–Mo systems was extended to the Pd–Mo/Al_2O_3 system, and nitrogen spillover was observed again[11].

CONCLUSIONS

FEM and FIM results have shown that energy dissipation and surface mobility are decisive factors influencing catalysis by metals in general and processes of model catalysts preparation in particular. Most of the hitherto observed surface phenomena on transition metals can be understood in terms of the above described model (Fig. 3). This model was previously named the localized-delocalized electron interplay (LDEI) model (proposed[4,5] on the basis of FEM and FIM results). The following surface phenomena explainable by this model, were mentioned in this paper to demonstrate its general applicability: preferential trapping of particles from the gas phase at the atomic steps, surface reconstruction due to adsorption and/or surface reaction, recovery of trapping sites by surface migration of reactants or of their fragments along the atomically flat terraces, mapping of the trapping sites distribution in favourable cases from the initial shape and the time development of the reaction zone, and finally a weak bond of product molecules on flat terraces, enabling their easy desorption.

The support of this work by the Grant Agency of the Czech Republic (grants No. 203/96/0951 and No. 202/98/K002) is gratefully acknowledged. The authors express their thanks to Dr S. Cerny for the critical reading of the manuscript and to Ms M. Barvirova for technical assistance in its preparation.

REFERENCES

1. Halstead D., Holloway S.: *J. Chem. Phys.* **1990**, *93*, 2859.
2. Redhead P. A., Hobson J. P., Kornelsen E. V.: *The Physical Basis of Ultrahigh Vacuum*. Chapman and Hall, London 1968.
3. Knor Z.: *Collect. Czech. Chem. Commun.* **1979**, *44*, 3434; and references therein.
4. Knor Z.: *Surf. Sci.* **1978**, *70*, 286.
5. Knor Z. in: *Catalysis – Science and Technology* (J. R. Anderson and M. Boudart, Eds), Vol. 3, p. 231; and references therein. Springer, Berlin 1982.
6. Knor Z.: *Rec. Trav. Chim. Pays-Bas* **1994**, *113*, 439; and references therein.
7. Mingo N., Knor Z.: *Chem. Phys. Lett.* **1996**, *263*, 8.
8. Debb B. M.: *Rev. Mod. Phys.* **1973**, *45*, 22.
9. Somorjai G. A.: *Introduction to Surface Chemistry and Catalysis*. Wiley & Sons Inc., New York 1994.
10. Knor Z., Sotola J.: *Collect. Czech. Chem. Commun.* **1988**, *53*, 2399.

11. Sotola J., Knor Z.: *J. Catal.* **1994**, *145*, 501.
12. Holzl J. in: *Solid Surface Physics* (G. Hohler, Ed.), Springer Tracts in Modern Physics, Vol. 85, p. 45. Springer, Berlin 1979.
13. Dvorak L.: *Ph.D. Thesis.* J. Heyrovskÿ Institute of Physical Chemistry, Academy of Sciences of the Czech Republic, Prague 1996.
14. Kaye G. W. C., Laby T. H.: *Tables of Physical and Chemical Constants*, 15th ed. Longman, London 1993.
15. Muller E. W.: *Adv. Electron. Electron Phys.* **1960**, *13*, 83.
16. Harris I. R., Raynor G. V.: *J. Less-Common Met*. **1969**, *17*, 336.
17. Rao C. N., Rao K. K.: *Can. J. Phys*. **1964**, *42*, 1336.
18. Waseda Y., Hirata K., Ohtani M.: *High Temp. High Pressures* **1975**, *7*, 221.
19. Sotola J., Knor Z.: *Appl. Surf. Sci.* **1988**, *31*, 173.
20. Knor Z., Sotola J.: *Surf. Sci.* **1989**, *213*, 371.
21. Campbell Ch. T.: *Surf. Sci. Rep*. **1997**, *27*, 1.
22. Knor Z., Biehl St., Plsek J., Dvorak L., Edelmann Ch.: *Vacuum* **1998**, *51*, 11.
23. Gadzuk J. W., Plummer E. W.: *Rev. Mod. Phys.* **1973**, *45*, 487.
24. Sotola J., Knor Z.: *Collect. Czech. Chem. Commun.* **1993**, *58*, 2695.
25. Knor Z., Edelmann Ch., Rudny J., Stachurski J.: *Appl. Surf. Sci.* **1986**, *25*, 107.
26. Knor Z., Plsek J., Dvorak L.: *Collect. Czech. Chem. Commun.* **1997**, *62*, 213.
27. Gorodetskii V. V., Sobyanin V. A., Bulgakov N. N., Knor Z.: *Surf. Sci.* **1979**, *82*, 120.
28. Khobiar S., Peck R. E., Reitzer B. J.: *Proc. 3rd Int. Congr. on Catalysis, Amsterdam, July 20–25, 1964* (W. M. H. Sachtler, G. C. A. Schuit and P. Zwietering, Eds), Contribution I-12. North-Holland Publ. Co., Amsterdam 1965.
29. Ponec V., Knor Z., Cerny S.: Ref.[28], Contribution I-13.
30. Pajonk G. M.: *Heterog. Chem. Rev.* **1994**, *1*, 329.
31. Conner C. W., Jr., Falconer J. L.: *Chem. Rev.* **1995**, *95*, 759.
32. Knor Z., Lazarov D.: *Czech. J. Phys. B* **1966**, *16*, 333.
33. Couper A., John C. S.: *J. Chem. Soc., Faraday Trans. 1* **1971**, *73*, 961.